Received: 20 October 2021 | Accepted: 7 December 2021 | Revised: 7 December 2021

DOI: 10.1111/gcb.16046

Global Change Biology WILEY

RESEARCH ARTICLE

Reduced ecosystem resilience quantifies fine-scale heterogeneity in tropical forest mortality responses to drought

Donghai Wu[1] | German Vargas G.[2] | Jennifer S. Powers[2,3] | Nate G. McDowell[4,5] | Justin M. Becknell[6] | Daniel Pérez-Aviles[3] | David Medvigy[7] | Yanlan Liu[8] | Gabriel G. Katul[9] | Julio César Calvo-Alvarado[10] | Ana Calvo-Obando[10] | Arturo Sanchez-Azofeifa[11] | Xiangtao Xu[1]

[1]Department of Ecology and Evolutionary Biology, Cornell University, Ithaca, New York, USA

[2]Department of Plant and Microbial Biology, University of Minnesota, St. Paul, Minnesota, USA

[3]Department of Ecology, Evolution and Behavior, University of Minnesota, St. Paul, Minnesota, USA

[4]Atmospheric Sciences and Global Change Division, Pacific Northwest National Lab, Richland, Washington, USA

[5]School of Biological Sciences, Washington State University, Pullman, Washington, USA

[6]Environmental Studies Program, Colby College, Waterville, Maine, USA

[7]Department of Biological Sciences, University of Notre Dame, Notre Dame, Indiana, USA

[8]School of Earth Sciences, The Ohio State University, Columbus, Ohio, USA

[9]Department of Civil and Environmental Engineering and the Nicholas School of the Environment, Duke University, Durham, North Carolina, USA

[10]Escuela de Ing. Forestal, Instituto Tecnológico de Costa Rica, Barrio Los Ángeles, Cartago, Costa Rica

[11]Earth and Atmospheric Sciences Department, University of Alberta, Edmonton, AB, Canada

Correspondence
Dr. Donghai Wu and Xiangtao Xu, Department of Ecology and Evolutionary Biology, Cornell University, Ithaca, NY 14850, USA.
Emails: dw623@cornell.edu (D. W.) and xx286@cornell.edu (X. X.)

Funding information
National Science Foundation, Grant/Award Number: DEB-1053237; Cornell University; National Science and Engineering Research Council of Canada; U.S. Department of Energy, Office of Science, Terrestrial Ecosystem Science Program, Grant/Award Number: DE-SC0014363

Abstract

Sensitivity of forest mortality to drought in carbon-dense tropical forests remains fraught with uncertainty, while extreme droughts are predicted to be more frequent and intense. Here, the potential of temporal autocorrelation of high-frequency variability in Landsat Enhanced Vegetation Index (EVI), an indicator of ecosystem resilience, to predict spatial and temporal variations of forest biomass mortality is evaluated against in situ census observations for 64 site-year combinations in Costa Rican tropical dry forests during the 2015 ENSO drought. Temporal autocorrelation, within the optimal moving window of 24 months, demonstrated robust predictive power for in situ mortality (leave-one-out cross-validation $R^2 = 0.54$), which allows for estimates of annual biomass mortality patterns at 30 m resolution. Subsequent spatial analysis showed substantial fine-scale heterogeneity of forest mortality patterns, largely driven by drought intensity and ecosystem properties related to plant water use such as forest deciduousness and topography. Highly deciduous forest patches demonstrated much lower mortality sensitivity to drought stress than less deciduous forest patches after elevation was controlled. Our results highlight the potential of high-resolution remote sensing to "fingerprint" forest mortality and the significant role of ecosystem heterogeneity in forest biomass resistance to drought.

KEYWORDS
ecosystem resilience, EVI, extreme drought, forest mortality, remote sensing, spatial heterogeneity, tropical dry forests, vegetation index

1 | INTRODUCTION

Enhanced forest mortality driven by extreme drought can disturb ecosystem structure (Allen et al., 2015) and leave sustained negative effects on ecosystem functions (Rowland et al., 2015; Saatchi et al., 2013). Forest ecosystems might become more vulnerable to drought disturbances in future climate because many of them are experiencing chronic increases in water stress (Ault, 2020), fueled by increasing atmospheric water demand and intensifying extremes within the hydrological cycles (McDowell et al., 2018). Thus, sensitivity of forest mortality to water stress is becoming necessary for assessing forest vulnerability to future hydroclimatic changes (Brando et al., 2019; Feldpausch et al., 2016; McDowell et al., 2018, 2020; Young et al., 2017), especially in the biodiverse and carbon-dense tropical forests (Brando et al., 2019).

Despite an identified general positive drought–mortality relation in tropical forests from field census data during the 2005 Amazon drought (Phillips et al., 2010), the relation did not hold during the subsequent 2010 drought (Feldpausch et al., 2016). Some of the complexity in tropical forest mortality responses to drought might arise from plant functional diversity (Aleixo et al., 2019; Powers et al., 2020) and topography (Schwartz et al., 2019; Zuleta et al., 2017), which might vary at rather fine spatial scales. However, limited spatial coverage of tropical field plots and relatively infrequent census interval (e.g., 5 years) compared with the timescale of drought impacts (1–2 years) prohibit robust analyses on these biotic and abiotic determinants on the drought–mortality relation. In fact, quantification of drought-driven forest mortality and its spatial variability at fine scale has been and continues to be a daunting task (Anderegg et al., 2013; Hartmann et al., 2015).

Increasing availability and accessibility of remote sensing products provide new opportunities to fill in the data and knowledge gaps in tropical forest mortality. Microwave remote sensing, Light Detection and Ranging (LiDAR), and Synthetic Aperture Radar (SAR) are widely used to infer changes in aboveground forest biomass (Fan et al., 2019; Saatchi et al., 2013; Wigneron et al., 2020; Yang et al., 2018) but these available products are too coarse or data limited to quantify variations in drought–mortality relations. On the other hand, high-resolution remote sensing products mostly available from visible and near-infrared bands reflect regional ecosystem dynamics at similar spatial scales (tens of meters) as field observations and thus have potential to monitor spatial variations in forest mortality. Although these optical remote sensing data cannot be directly linked to biomass as LiDAR or microwave observations and can suffer from limited penetration depth and frequent cloud cover over tropical forests, they provide surrogate information for vegetation dynamics at the canopy top, which likely dominate forest biomass loss during drought (Bennett et al., 2015). However, few efforts (Anderegg et al., 2019; Baccini et al., 2017) integrate them to assess forest mortality or biomass changes in tropical forest and none of them assessed the determinants of spatial heterogeneity in drought–mortality relations.

In addition to analyzing the anomaly and trends in remote sensing signals (Rogers et al., 2018), quantifying drought-driven forest mortality from remote sensing observations can benefit from the theory of critical transition in complex systems (Scheffer et al., 2012; Strogatz, 2018). Under water stress, plants usually experience reduced resilience due to compromised ecophysiology such as stomatal closure, leaf shedding, and hydraulic failure. At the ecosystem level, individual-level stress can manifest as reduced ecosystem resilience defined as slower recovery of ecosystem states from perturbations. Reduced resilience indicates that ecosystem is moving toward the point of critical slowing down (Scheffer et al., 2012) that can lead to abrupt transition to an alternative stable state (e.g., from forest to savanna ecosystems) (Hirota et al., 2011; Staver et al., 2011). The degree of reduced resilience can be quantified using lag-1 temporal autocorrelation of ecosystem states after removing low-frequency variability (Verbesselt et al., 2016) because ecosystem state correlates more with its previous state under lower recovery rate. Therefore, the autocorrelation of remotely sensed vegetation index is able to provide early warning signals of ecosystem tipping point such as forest dieback (Liu et al., 2019). However, it remains unclear whether ecosystem resilience based on autocorrelation in vegetation index can quantitatively reflect the magnitude of ecosystem changes before tipping points such as partial forest biomass loss in tropical forests during droughts.

In 2015, an extreme El Niño-Southern Oscillation (ENSO) associated drought hit global tropical ecosystems (Castro et al., 2018; Cooley et al., 2019; Liu et al., 2017). In the hard-stricken tropical dry forests in northwest Costa Rica with more than 30% reduction in annual rainfall (Figure S1), long-term annual forest inventory census records suggested that the average plot-level mortality in 2015 (6%) was elevated relative to background mortality (3%) (Powers et al., 2020). These observations provide a unique opportunity to bridge remotely sensed ecosystem resilience and forest mortality because the scale of the field plots (1000 m^2) is commensurate to Landsat satellite products (~900 m^2). The resulting estimates of fine-scale spatial variations in forest mortality can also enhance our understanding in the drivers of forest mortality heterogeneity under extreme droughts.

Here, we aim to first evaluate the hypothesis that lag-1 autocorrelation of high-frequency variability in Landsat Enhanced Vegetation Index (EVI) can predict in situ forest biomass mortality over Costa Rican tropical dry forests. Subsequently, we investigate the sources of fine-scale heterogeneity in drought–mortality

relations revealed from the 30 m resolution EVI data. Specifically, we hypothesize that biotic factors such as forest deciduousness and abiotic factors such as topography, which all influence plant water use, are dominant drivers of mortality heterogeneity aside from drought intensity.

2 | MATERIALS AND METHODS

2.1 | Field observations

We used 64 in situ census observations from sixteen 0.1 ha long-term forest plots in Costa Rica covering the drought period from 2014 to 2017 (Table S1). The plots are representative of forest heterogeneity and topography across low land dry forests in northwest Costa Rica (Table S2). All trees with diameter at breast height (DBH) larger than 10 cm were censused annually at the end of wet season (Powers et al., 2020). An allometric biomass model is used to estimate aboveground biomass from observed DBH and wood-specific gravity (van Breugel et al., 2011). We assessed relative forest mortality using proportional loss of aboveground forest biomass (AGB) as the difference between $\log_e(AGB_{t-1})$ and $\log_e(AGB_t)$ where t represents any given year in the study period.

2.2 | Landsat EVI residual autocorrelation

To establish the relation between the remote sensing vegetation index and field plots, we used 30 m resolution monthly Landsat EVI for Costa Rica from Google Earth Engine. Here, EVI time series is based on the USGS Landsat 7 surface reflectance tier 1 product from 1999 to 2019 and Landsat 8 surface reflectance tier 1 product from 2013 to 2019. Data quality control was applied by removing the observations affected by cloud and cloud shadow. Monthly EVI was then produced via the maximum value composite method with more than one observation in a month. Because overlapped measurements from Landsat 7 and Landsat 8 are significantly correlated (correlation coefficient $R \approx 0.9$ among the field plots), we combined EVI time series of Landsat 7 and Landsat 8 by correcting the system bias between the two sensors using linear regression.

EVI represents the greenness of forest canopy, which is the composite of forest structure (maximum canopy green area) and phenology (fullness of canopy cover). In the tropical dry forests in Costa Rica, EVI displays strong seasonality and is highly correlated with precipitation based on ground meteorological stations in pre-drought years during 1999 and 2014 (mean $R^2 = 0.72$ across the field sites). Such recurring longer-term variation must be removed to infer the ecosystem resilience through lag-1 autocorrelation (Liu et al., 2019; Verbesselt et al., 2016). Therefore, we decomposed the seasonal and inter-annual variations in EVI as follows:

$$\log_e(EVI_t) = \log_e(EVI_0) + b \times \log_e\left(\sum P_t\right) + \varepsilon_t, \quad (1)$$

where EVI_t denotes raw monthly EVI values at monthly time t, EVI_0 represents a reference EVI value for the forest patch, $\sum P_t$ represents the 3-month cumulative rainfall from month t-2 to month t, b is the phenological sensitivity of EVI to rainfall variations, and ε_t is the residual term that incorporates forest structural changes and other noise not accounted for by Equation 1. Three-month cumulative rainfall was used because it has the best correlation with EVI. The two unknown parameters EVI_0 and b were estimated by regressing EVI against $\sum P_t$ using observations during pre-drought years (1999–2014). We then removed seasonal and inter-annual variations in EVI using the relation with $\sum P_t$ for all years including the 2015 ENSO drought years and obtained time series of ε_t that represent high-frequency variability of EVI (see an example from one field site in Figure 1a). Here, log-transformed EVI are used so that the changes in residual (ε_t) can be directly linked to the relative forest mortality. Using EVI residual without log-transformation led to qualitatively similar results yet reduced predictive performance in the subsequent analyses. Therefore, only log-transformed results are reported.

Finally, we treated the magnitude of EVI residual autocorrelation (without filling the missing observations) as a predictor for forest biomass mortality and tested our first hypothesis by evaluating the relation between ε_t autocorrelation and in situ forest biomass mortality across space and time. In accordance with the annual census data, we used the mean value of ε_t autocorrelation of 12 consecutive months corresponding to each observation year. We explored how the selection of the rolling temporal window influences the relation by evaluating the Pearson correlation coefficient across different moving windows (12–36 months) and lags (12 months in advance to 12 months later). In addition, we also compared the predictive performance of ε_t autocorrelation with the performance of two additional traditional metrics: EVI residual trend and EVI residual mean. Based on our method, EVI residual mean incorporates forest structural changes and other noise; and EVI residual trend is considered as the trend of forest structural changes. Here, EVI residual mean and EVI residual trend are supposed to be negatively correlated with forest mortality rates.

2.3 | Estimation of regional forest mortality and its determinants

Before estimating the spatial patterns of forest mortality, we performed three types of cross-validation based on datasets from original and six additional forest census plots from other group (i.e., TROPI-DRY) (Calvo-Rodriguez et al., 2021; Hilje et al., 2015) to testify the robustness of the optimal relation between EVI autocorrelation and forest mortality. Then, based on the best relation at plot level, we generated the spatial map of forest biomass mortality from Landsat EVI residuals autocorrelation during 2014–2017. To remove regular seasonal and inter-annual variability in EVI due to water availability in the same way as our plot-level analysis, we used a quasi-global (50°S–50°N) monthly precipitation dataset, Climate Hazards

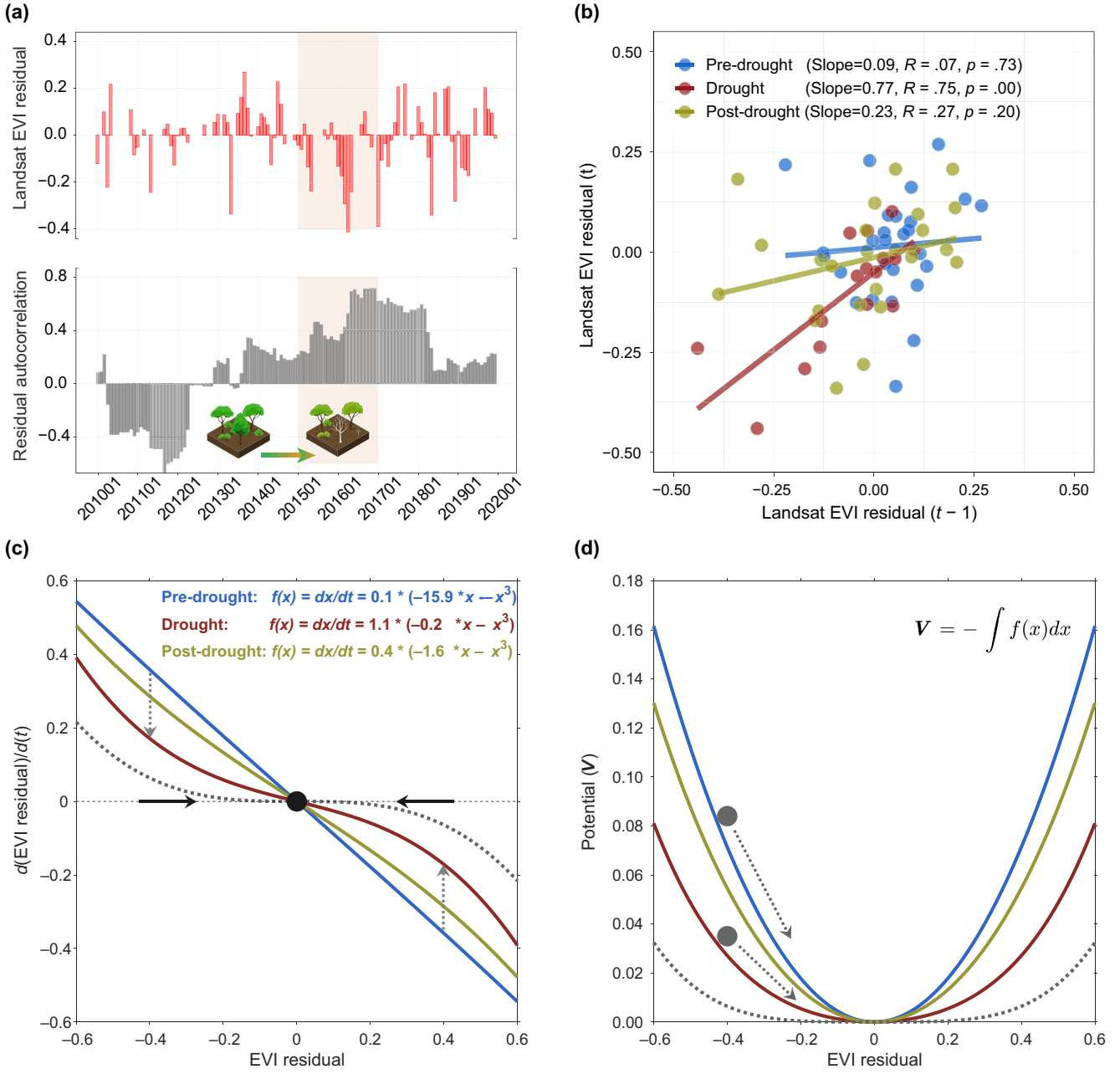

FIGURE 1 Example of EVI residual autocorrelation. The Landsat EVI time series represent one field site in Sector Santa Rosa with high biomass mortality during the 2015 drought. (a) EVI residual (red bar) time series in upper subplot and lag-1 residual autocorrelation of 24-month moving windows (gray bars) in lower subplot. Here, EVI residual time series is calculated by removing the long-term phenological responses of EVI to precipitation. EVI residual time series, after removing the seasonality (see Figure S8 for raw time series), mainly incorporates information on forest structural changes. (b) Linear regression between EVI residual (t–1) and EVI residual (t) for pre-drought (2010–2014), drought (2015–2016) and post-drought (2017–2019) periods. Higher regression slope and R during drought period imply that the forest ecosystem became less resilient and much more dependent on its previous time state. (c) Relations between EVI residual and its change rate for pre-drought, drought, and post-drought periods. Each color solid line shows a third-order nonlinear dynamical model (a general form for quantifying system resilience, see Figure S9 for details) fitted with observed EVI residuals across the 16 sites. The black dot is a stable point at EVI residual = 0, which represents an equilibrium of the forest ecosystem. Grey dotted line represents the theoretical dynamics when ecosystem state reaches critical slowing down ($f(x) = -x^3$) and the recovery rate becomes much slower. Grey dotted arrows show the ecosystem moved toward the critical slowing down during the extreme drought. (d) Relations between EVI residual and its potential, defined as the negative integral of $f(x)$, for pre-drought, drought, and post-drought. The basin of attraction become shallower during drought compared with the pre-drought, which indicates reduced ecosystem resilience associated with decreased recovery rate and increased autocorrelation. Grey balls and corresponding dotted arrows illustrate the recovery rates under normal and drought conditions

Group InfraRed Precipitation with Station data (CHIRPS), which has high spatial resolution (0.05°), covers 1981 to near-present (Funk et al., 2015) and shows high correlation with ground-based precipitation across our sites (Figure S2).

To explore the environmental drivers of spatial patterns of forest biomass mortality in response to the ENSO drought event, we used topography datasets (elevation, aspect, slope, and topographic wetness index) based on the Shuttle Radar Topography Mission (SRTM) digital elevation data (Farr et al., 2007) with spatial resolution of 30 m area used as environmental drivers as well. Here, the aspect and slope were derived from Google Earth Engine, and topographic wetness index was derived via ArcMAP 10.2 based on elevation data. In addition, CHIRPS precipitation was used to calculate monthly cumulative water deficit (CWD), an indicator of drought stress (Phillips et al., 2010), by assuming an average potential evapotranspiration of 75 mm per month estimated from a process-based terrestrial biosphere model (Xu et al., 2016). CWD rather than vapor pressure deficit (VPD), an indicator for atmospheric drought stress on vegetation (Grossiord et al., 2020), was used because data quality of VPD is low in tropical forests due to scarce ground-based measurements (Abatzoglou et al., 2018) and VPD, rainfall, and CWD are usually highly correlated during extreme droughts like the 2015 ENSO drought at monthly scale.

To avoid spurious signals in autocorrelation, we excluded grids with relative precipitation reduction in 2015 <30% (Figure S1), forest cover <50% (Figure S3c), crop cover >10% (Figure S3d), or total valid EVI observations <50 (Figure S4). Furthermore, we also performed sensitivity analyses for the threshold settings in results. We used the forest cover dataset from Copernicus Global Land Cover Layers with spatial resolution of 100 m (CGLS-LC100V2). To match the geographic location of Landsat EVI, we resampled all other datasets to spatial resolution of 30 m using a nearest neighbor method.

Because our analysis relates EVI residual autocorrelation with relative biomass mortality, we further estimated the spatial patterns of absolute aboveground biomass loss in 2015 based on the Global Forest Watch aboveground biomass product (https://data.globalforestwatch.org/). This data product provides a global map of AGB with a spatial resolution of 30 m, and the biomass map matches with in situ observed pre-drought AGB (Figure S5).

To evaluate our second hypothesis on the determinants of forest mortality heterogeneity, we first assessed the sensitivity of forest mortality to annual average CWD anomaly (Figure S6). We performed linear weighted regression analysis (Phillips et al., 2010) using the estimated annual forest mortality across valid grid cells during 2014–2017 in each 5 mm interval of annual average CWD anomaly from −100 mm to 0 mm. We further compared regression results from subsets of grid cell with different forest deciduousness and elevation (Figures S3 and S7), two major factors influencing ecosystem water use and stress in our study region. Here, deciduousness is calculated as the ratio between the average seasonal EVI amplitude (EVI_{max} − EVI_{min}) and the maximum EVI.

Aside from deciduousness and elevation, other environmental drivers (e.g., slope, aspect, maximum greenness, forest cover, and topographic wetness index) may also contribute to the heterogeneous patterns. Therefore, we investigated the determinants of spatial heterogeneity in forest mortality during 2014–2017 when the meteorological drought hit the study region homogeneously and their potentially nonlinear effects using boosted regression trees (BRT). The BRT method combines the advantages of regression trees and boosting and can establish robust relations between dependent and independent variables without any a priori assumptions (Elith et al., 2008). In this analysis, we include deciduousness (Figure S3a), maximum EVI (Figure S3b), forest cover (Figure S3c), CWD anomaly (Figure S6), elevation (Figure S7a), aspect (Figure S7b), slope (Figure S7c), and topographic wetness index (Figure S7d). In addition to a BRT analysis over all valid grid cells across our whole study region, we also applied the BRT on local windows of 900 m by 900 m to examine potential local variations in the relative importance of the environmental determinants. For the local BRT analysis, CWD was excluded because the rainfall dataset is too coarse to characterize heterogeneity at such scale. We extracted the cross-validation performance, variable importance, and partial dependence of each variable for all BRT analyses.

3 | RESULTS

3.1 | Relation between EVI autocorrelation and forest mortality

The lag-1 autocorrelation of EVI residual (ε_t) within a given rolling time window was calculated to infer whether it is increasing during drought period. As an example, ε_t autocorrelation within 24 months moving window before the current month increased during the 2015 ENSO drought at one of the field sites in Sector Santa Rosa of Costa Rica (Figure 1a, Figure S8), where high mortality rate (Site 4, 0.39 yr^{-1} in 2015 and 0.61 yr^{-1} in 2016, Table S1) was observed. Such autocorrelation increases indicated reduced ecosystem resilience and corresponded to enhance dependence of EVI high-frequency variability on its previous state as demonstrated by the changes in linear regression slopes between ε_t and ε_{t-1} for pre-drought, drought, and post-drought periods (Figure 1b). Across all forest plots considered, the recovery rate of EVI residual under a given EVI residual anomaly (i.e., a perturbation) became lower during the drought compared with both pre-drought and post-drought periods (Figure 1c) and its corresponding basin of attraction became shallower (Figure 1d). These changes in EVI dynamics suggest that increases in EVI residual autocorrelation indeed reflected the predisposition of critical slowing down (Liu et al., 2019; Scheffer et al., 2009; Strogatz, 2018) over the forest plots during the drought (see Figure S9 for details of the nonlinear dynamical model).

We then applied the methods to all 16 census plots around the drought period (2014–2017). The correlation between EVI residual autocorrelation and 64 in situ forest mortality observations generally increased with the length of moving window before reaching ~24 months (Figure 2a). The correlation was weaker

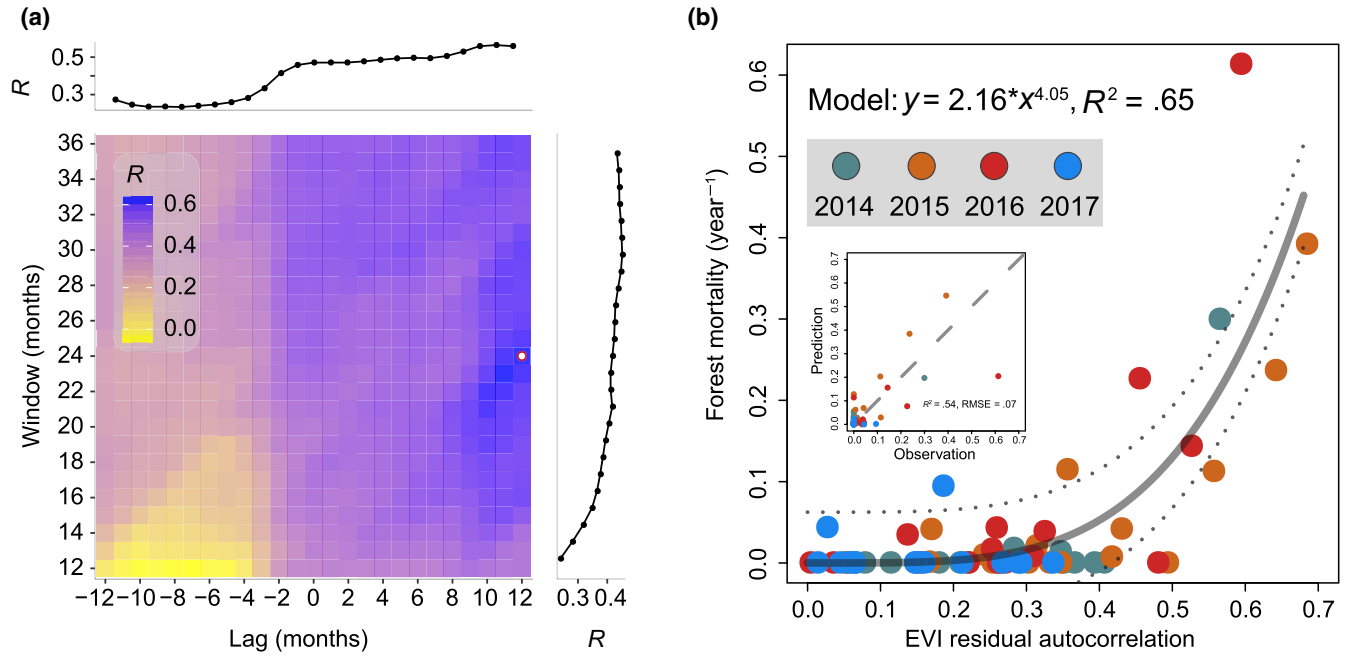

FIGURE 2 Relations between Landsat EVI residual autocorrelation and in situ forest mortality. (a) The Pearson correlation coefficient between autocorrelation and forest mortality across different moving windows and lags. The axis at the upper margin represents the mean correlation of all moving windows in each lag interval. The axis at the right margin represents the mean correlation of all lags in each moving window interval. Moving window of 24 months and lag of post 12 months led to the best performance ($R = 0.61$, white dot with red edge). (b) After fitting to a power law model (solid line with the 95% confidence intervals outlined as dotted lines), the residual autocorrelation explained 65% of the observed forest mortality spatiotemporal variations. Each dot represents mortality of in situ records (16 plots from 2014 to 2017) and the color of the dot represents observation year. The 2 years with peak mortality (2015 and 2016) are labeled with orange and red, respectively. The inset shows the leave-one-out cross-validation for the optimal relation. Other two types of cross validation based on datasets from original and additional annual forest census plots are performed to further testify the robustness of the optimal relation (see Figures S15–S17)

for moving windows with negative time lags (i.e., only using EVI advancing observed forest mortality events), whereas the correlation increased for moving windows with positive lags (i.e., using EVI including observed forest mortality events). We found the optimal moving window ($R = 0.61$) has a length of 24 months and time lag of +12 months (Figure 2a), which incorporates EVI observations from the drought year as well as the year before and year after.

After fitting a power law model, the residual autocorrelation explained 65% of the observed forest mortality spatiotemporal variations across 16 field sites (Figure 2b). The relation was highly nonlinear with forest mortality markedly increasing when autocorrelation exceeds 0.4, which suggests that the forest's resilience may move close to the point of critical slowing down (Scheffer et al., 2012). The relation remained robust but has a lower R^2 value of 0.61 if we used EVI residual in linear space (Figure S10). For the other two metrics, including EVI residual trend and annual mean EVI residual, there were no statistically significant relations with in situ mortality (Figures S11 and S12). In addition, we performed similar analyses with two additional vegetation indices (normalized difference vegetation index, NDVI and near-infrared reflectance of vegetation, NIRV); however, the optimal relations are much weaker than the relation with EVI (Figures S13 and S14). Thus, EVI residual autocorrelation is used as the optimal choice for generating forest mortality map at the regional scale.

To further testify the robustness of the optimal relationship between EVI autocorrelation and forest mortality, we performed three types of cross-validation based on datasets from original and new annual forest census plots. First, we conducted leave-one-out cross-validation using the original dataset under the optimal temporal window (Figure 2b). Results suggested that the cross-validation relationship is robust ($R^2 = 0.54$, RMSE = 0.07). Second, we validated the relationship with 24 additional in situ census observations across six additional 0.1 ha census plots in Costa Rica from TROPI-DRY plots (Calvo-Rodriguez et al., 2021; Hilje et al., 2015). Results suggested that the mortality–resilience relationship generated from our original dataset can also capture the observed mortality ($R^2 = 0.51$, RMSE = 0.03) during the drought period of the new sites (Figure S15). Third, we evaluate whether the relationship between forest mortality and remotely sensed resilience can be extrapolated spatially by subdividing our datasets to Sector Santa Rosa (Northwest) and Palo Verde (Southwest) (Ploton et al., 2020), which are ~70 km apart and have different soil characteristics and vegetation composition (Powers et al., 2009). We calibrated the relationship using data from Sector Santa Rosa, which was then contrasted with data from Palo Verde (Figure S16). Results suggested that the relationship is

still robust (R^2 = 0.47, RMSE = 0.03). However, when we built the relationship using datasets from Palo Verde and validated with datasets from Sector Santa Rosa (Figure S17), the relation was still strong but systematically underestimate the forest mortality in Santa Rosa (R^2 = 0.52, RMSE = 0.09) because the lack of high mortality observations in Palo Verde (max mortality 0.11 compared with max mortality 0.61 in Santa Rosa) left the mortality–resilience relationship unconstrained at the higher end. Our results suggest that spatial extrapolation should be robust as long as the training dataset incorporates a wide range of forest mortality rates, at least over Costa Rica.

3.2 | Regional forest mortality patterns

Based on the best relations between residual autocorrelation and field forest mortality (Figure 2b), we generated relative forest mortality maps for northwestern Costa Rica from 2014 to 2017 at 30 m resolution (Figure 3a). In 2015, the peak of drought, 69% of the forested area (forest cover >50%) displayed mortality rates lower than 0.03 yr^{-1}, and 15% experienced relative biomass mortality rates greater than 0.1 yr^{-1}. The highest forest mortality rates occurred at Sector Santa Rosa in the northern part of our study region, with values close to 0.2 yr^{-1}. We find that forest biomass mortality was generally higher but more variable across space in mountainous regions (e.g., 0.06 ± 0.12 yr^{-1} in regions with elevation >500 m) than lowland forests (e.g., 0.04 ± 0.09 yr^{-1} in regions with elevation <100 m) (Figure 3a). Combining the aboveground biomass map from the Global Forest Watch dataset, we estimated the total aboveground biomass loss in 2015 to be about 1.4 Tg (~0.9 kg m^{-2}) in northwestern Costa Rican dry forests (Figure 3b), which is about 5.3% of the total aboveground biomass in our study region. The spatial variation in aboveground biomass loss largely follows the pattern of forest mortality.

The mean value of forest mortality across all forested areas in the study region peaked in 2015 and 2016 (0.05 yr^{-1}), compared with the mortality rates before (0.03 yr^{-1} in 2014) and after the drought (0.04 yr^{-1} in 2017) (Figure 3a). Magnitudes of the regional mean forest mortality are insensitive to the threshold settings for forest cover and valid EVI observations (Figure S18). The interannual variation in mortality was much higher at the hard-stricken Sector Santa Rosa (inset in Figure 3a). In this 0.1°-by-0.1° area, background mortality before the drought was ~0.01 yr^{-1}, which increased to 0.11 yr^{-1} and 0.08 yr^{-1} in 2015 and 2016. In 2017, mortality declined to 0.04 yr^{-1}, which is still higher than (p < .05) pre-drought values, suggesting some legacy effects of the drought impact.

3.3 | Drivers of fine-scale heterogeneity in forest mortality

To test whether topography and deciduousness regulate mortality sensitivity to drought, we first investigated the forest mortality sensitivity to cumulative water deficit (CWD) anomaly for forest patches at different elevations (Figure 4a, b). The regression slope between mortality and CWD is −0.0003 yr^{-1} mm^{-1} for low elevation (<300 m) forests, which is more negative than the slope for high elevation (−0.0002 yr^{-1} mm^{-1}, >300 m) while the regression intercept is larger for higher elevation forests (0.04 yr^{-1} vs. 0.02 yr^{-1}). This result

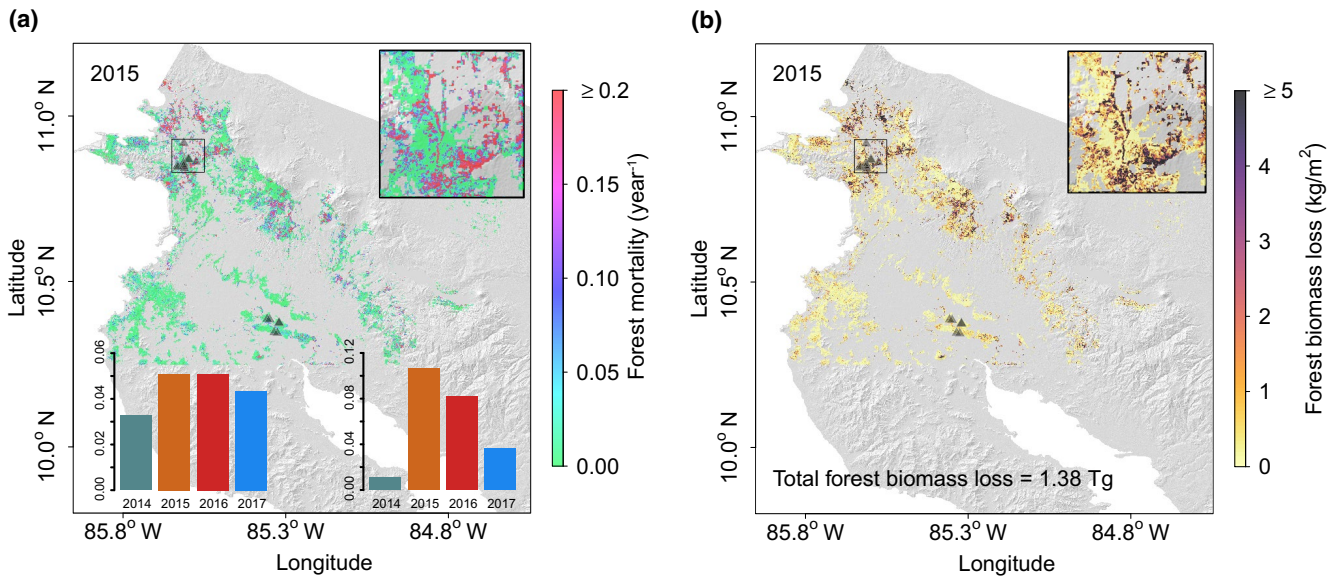

FIGURE 3 Heterogeneity in forest mortality and aboveground biomass loss at 30 m resolution in northwestern Costa Rica in 2015. (a) Forest mortality in Costa Rica in 2015. The lower left inset demonstrates the mean values of forest mortality during 2014 and 2017 for the whole regions, and the lower right demonstrates for the inset map of the focal in region at Sector Santa Rosa. (b) Forest aboveground biomass loss in Costa Rica in 2015 based on biomass map from Global Forest Watch. Black triangles represent 16 field plots at Sector Santa Rosa (northern sites, number = 10) and at Palo Verde National Park (southern sites, number = 6). The upper right insets are zoom-in maps (0.1°-by-0.1°) of the heterogeneous patterns in Sector Santa Rosa

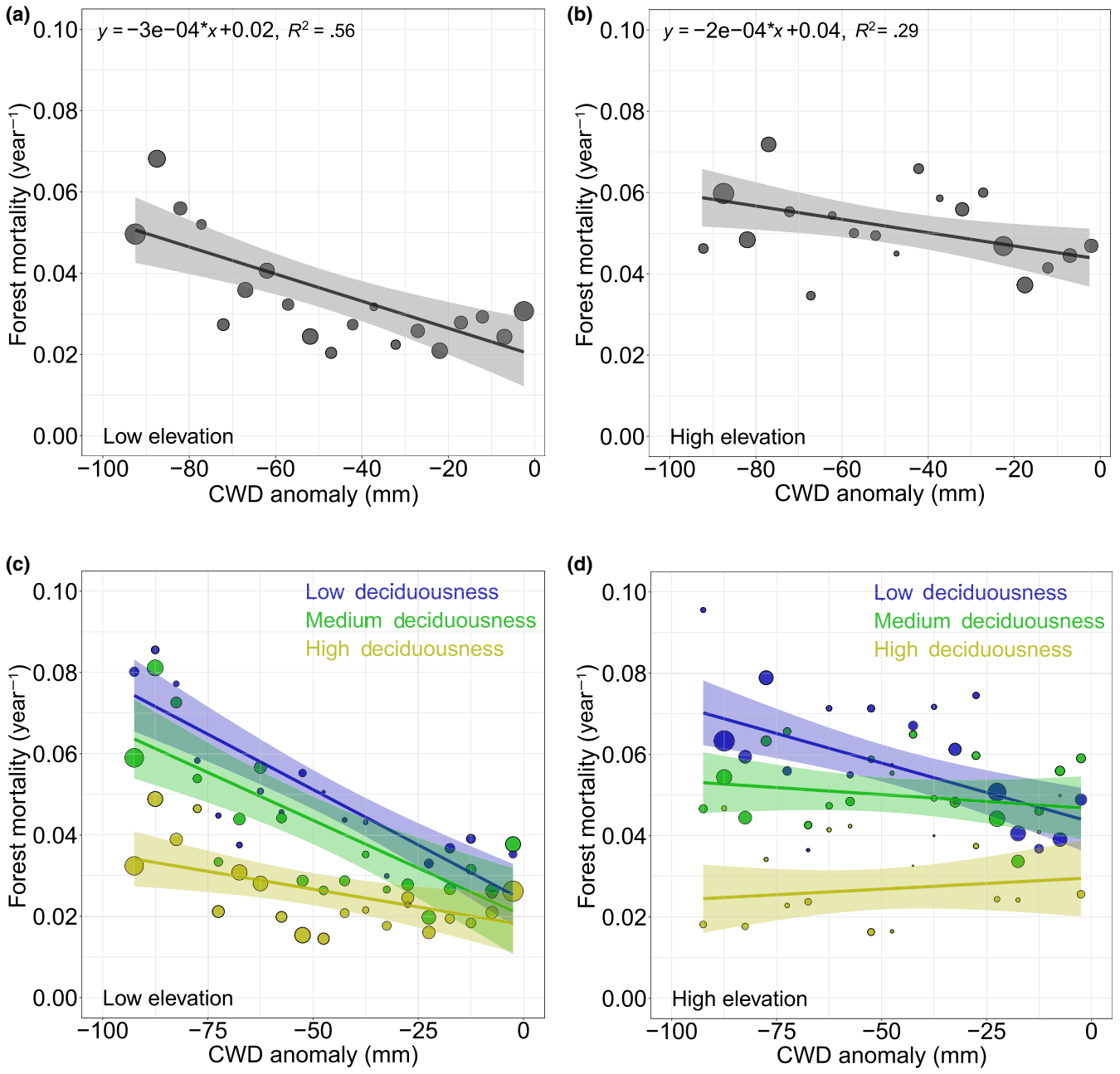

FIGURE 4 Sensitivity of forest mortality to cumulative water deficit (CWD) anomaly. Different sizes of plots represent relative magnitude of samples in binned CWD anomaly intervals. Linear weighted regressions are established for low elevation (a) and high elevation (b). (c, d) Regression results from subgroups of grid cells based on different forest deciduousness (<0.4 for low deciduousness, 0.4–0.6 for medium deciduousness, and >0.6 for high deciduousness). In (c), the regression results are $y = -5.451e\text{-}04^*x + 2.393e\text{-}02$, $R^2 = 0.78$, for low deciduousness, $y = -4.708e\text{-}04^*x + 2.009e\text{-}02$, $R^2 = 0.63$, for medium deciduousness, and $y = -1.753e\text{-}04^*x + 1.791e\text{-}02$, $R^2 = 0.33$ for high deciduousness. In (d), results are $y = -2.905e\text{-}04^*x + 4.337e\text{-}02$, $R^2 = 0.52$ for low deciduousness, $y = -6.859e\text{-}05^*x + 4.671e\text{-}02$, $R^2 = 0.06$ for medium deciduousness, and $y = 5.539e\text{-}05^*x + 2.964e\text{-}02$, $R^2 = 0.03$ for high deciduousness

suggests that forest mortality is more sensitive to drought stress (i.e., regression slope to CWD) in lower elevation forest, despite a lower baseline mortality rate under no water stress.

The evaluation of the deciduousness effect has been rare because of the lack of high-resolution mortality data across a deciduousness gradient under the same drought. Based on the high-resolution mortality maps and forest deciduousness derived from average EVI seasonal amplitude, we examined sub-groups of forest patches with different degrees of deciduousness for both low elevation and high elevation (Figure 4c, d). At low elevation, linear weighted regressions revealed that forest patches with low deciduousness (<0.4) is more sensitive to drought stress (−0.0005 yr^{-1} mm^{-1}) than with high deciduousness (>0.6, −0.0002 yr^{-1} mm^{-1}). By contrast, at high elevation, forest patches with low deciduousness still show relative high sensitivity to drought stress (−0.0003 yr^{-1} mm^{-1}), while forest patches with medium and high deciduousness are insensitive to water stress

(or CWD). Overall, the results indicated that highly deciduous forest patches have much lower mortality sensitivity in response to drought stress compared with evergreen forest patches regardless of elevation.

When all 5.3 million forested 30 m grid cells in the study region during 2014–2017 were included, the BRT model to explain the variation of forest biomass mortality yielded a cross-validation correlation of 0.5. As expected, drought intensity, represented by CWD anomaly, was the most important variable that controls spatial variations in mortality (Figure 5) with a relative importance score of 58%. The BRT results further suggested that forest mortality only increased by 0.01 yr^{-1} on average when CWD anomaly decreased from 0 mm to −70 mm, whereas forest mortality showed a much higher increase of 0.03 yr^{-1} from −70 mm to −90 mm (Figure 5a). The nonlinear sensitivity implies that −70 mm of CWD anomaly may be close to mortality threshold in tropical dry forests.

Consistent with our linear regression analyses (Figure 4), deciduousness and elevation were major determinants of forest mortality responses following water stress, with relative importance values of 17.9% and 10.6%, respectively. More evergreen forest patches (deciduousness <0.4) could experience 0.03 yr^{-1} higher mortality than more deciduous forest patches (deciduousness >0.7) if other conditions are the same (Figure 5b). Meanwhile, the sensitivity of mortality to elevation was relatively small. Mortality only increases by ~0.01 yr^{-1} from sea level to 600 m (Figure 5c). Aside from these two drivers, mortality could increase by 0.01 yr^{-1} for forest patches with very high maximum EVI (>0.65) and increase by 0.03 yr^{-1} for forest patches on steep slopes (Figure 5d). Forest mortality is relatively insensitive to other factors considered in the analyses, including aspect, forest cover, and topographic wetness index.

4 | DISCUSSION

4.1 | Predict forest biomass mortality from reduced ecosystem resilience

Separating forest ecosystem productivity and mortality from remote sensing has been challenging (Mitchard, 2018). The analysis here extends previous explorations in estimating mortality using high-resolution vegetation index (Anderegg et al., 2019; Huang & Anderegg, 2012; Liu et al., 2019; Rogers et al., 2018) and demonstrates that lag-1 temporal autocorrelation of high-frequency variability in Landsat EVI can be a predictor for forest biomass mortality

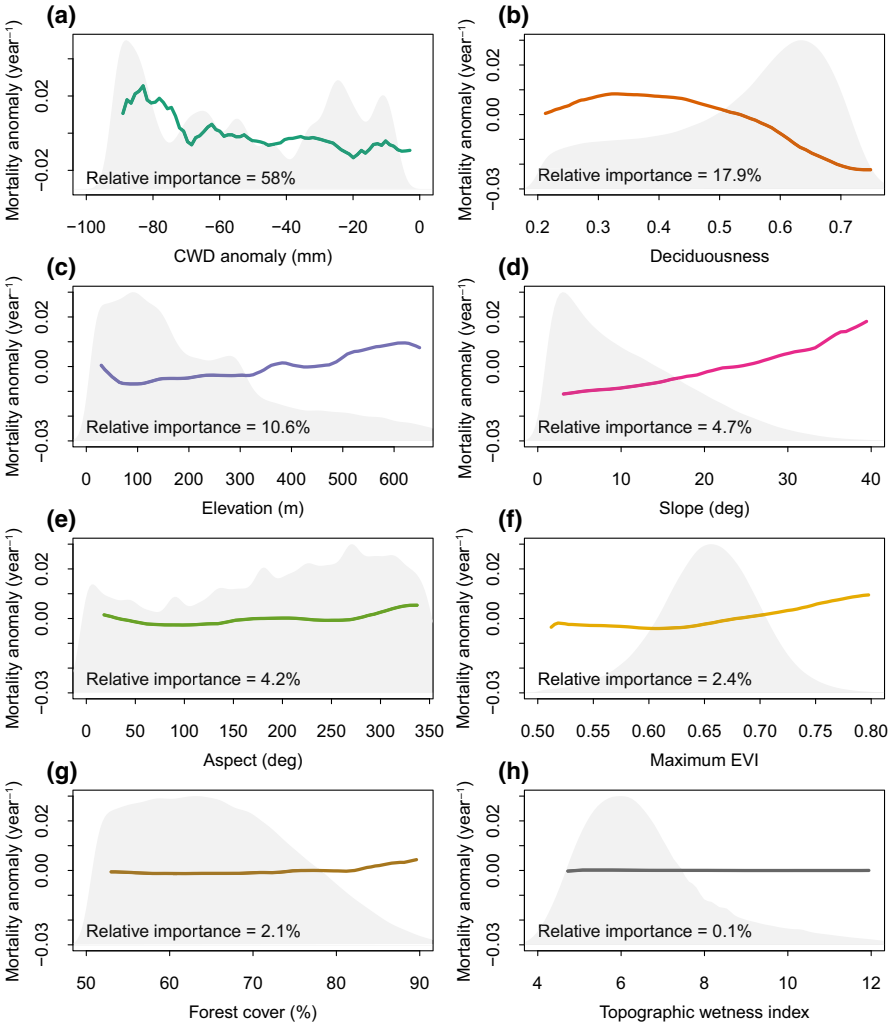

FIGURE 5 Sensitivity of forest mortality to environmental factors in Costa Rica. Each panel shows the partial dependence of mortality to one environmental variable after controlling for other factors based on the boosted regression tree results. Here, the partial dependence of forest mortality was centered to have zero mean over the data ranges and smoothed with moving window of size five to describe a general trend. Environmental factors include (a) annual mean cumulative water deficit (CWD) anomaly, (b) deciduousness, (c) elevation, (d) slope, (e) aspect, (f) maximum EVI, (g) forest cover, and (h) topographic wetness index. The total number of samples is 5.3 million during 2014–2017, and cross-validation correlation of the boosted regression trees is 0.5. Background colored grey is density map for each environmental variable

over tropical dry forests. However, we did not find strong early warning signals before forest mortality events during the 2015 ENSO drought given the relation between annual mean autocorrelation and in situ mortality rates was much worse when using a rolling time window preceding the observed mortality events (yellow regions in Figure 2a). By contrast, previous studies found early warning signals in 1.5 years ahead forest mortality for Californian forests (Liu et al., 2019), 5 years for Amazon lowland forests (Anderegg et al., 2019), and even more than 10 years for boreal forests (Rogers et al., 2018). The lack of early warning signals is not entirely surprising because the 2015 ENSO drought in Costa Rica was a relatively acute event. Trees likely received intense drought stress that led to mass mortality within a short period of time. Thus, the early warning signals might appear in just several months or weeks ahead of mortality, which cannot be detected using monthly remote sensing data and annual census. To detect early warning signals of forest mortality at monthly scales, high temporal resolution remote sensing (e.g., daily) coupled with frequent sub-annual censuses on field plots is required.

The identified optimal time window to quantify mortality rates using EVI autocorrelation suggests that 24 months can provide enough qualified data to characterize tropical forest responses to drought extremes. More interestingly, including EVI during and/or after the major drought impacts (positive time lags in Figure 2a) can greatly improve the relation between EVI autocorrelation and in situ mortality rates. This finding suggests that the recovery trajectory after the immediate drought impact (Schwalm et al., 2017; Yang et al., 2021) can enable quantifying the severity of the impact such as biomass mortality rates. A plausible explanation is that forests that experienced higher mortality can show more consistent post-drought recovery in leaf area, which increases ecosystem memory of previous state and thus temporal autocorrelation. Nevertheless, we expect the optimal time windows to predict forest mortality might vary across space and time because the time scale of the forest mortality responses and the subsequent recovery can change from a few months to decades, influenced by intrinsic forest resilience (Verbesselt et al., 2016), drought properties (e.g., chronic and episodic drought) (Allen et al., 2017), and local environment.

Overall, the results here provide evidence that high spatial resolution EVI time series can bridge plot to regional scales and offer diagnostics on tropical forest mortality. Particularly, we showed that the temporal autocorrelation of high-frequency EVI variability provided more robust predictive performance than anomaly or trends, which might be more susceptible to noise and data availability. This novel approach is based on reduced resilience of plants under external stress and might help to constrain forest mortality from stressors other than droughts that influence plant resilience such as insect attack (Anderegg et al., 2015; Raffa et al., 2008). However, it may be difficult to link the ecosystem resilience to forest mortality induced by acute disturbances such as fire and hurricane because forest system usually moves across the tipping point in a short time.

4.2 | Ecosystem heterogeneity drives forest mortality responses to drought

The integration of Landsat EVI and in situ mortality in our study provided an unprecedented high-resolution map of forest drought mortality for Costa Rican tropical dry forests. The relation still held robust when we used absolute forest biomass loss defined as the difference between AGB_{t-1} and AGB_t (Figure S19a), which can be used to directly estimate the absolute forest biomass mortality. This alternative method estimates the total absolute forest biomass loss in 2015 is 1.02 Tg (Figure S19b). This loss is comparable to the estimates based on relative forest mortality and Global Forest Watch AGB (1.38 Tg, Figure 3b).

Furthermore, we also found the patterns of residual autocorrelation and biomass loss in drought years are similar with Landsat when using EVI from the MOD13Q1 product with moderate resolution (Figure S20). Across our study region, the mean forest mortality in 2015 derived from MODIS EVI (0.04 yr^{-1}) is smaller than that derived from Landsat (0.05 yr^{-1}) (Figure S20), which may be induced by neutralization of the heterogeneity when using coarse resolution dataset. These findings demonstrate that MODIS EVI is also capable of identifying the changes of ecosystem resilience in response to extreme drought. Therefore, the resilience signals from different remote sensing platforms are robust, and in future studies, MODIS EVI time series may be useful to extend as auxiliary data for exploring the forest resilience and mortality on continental scale. The consistency also provides additional support for the robustness of the estimated regional forest mortality patterns.

These new data revealed large heterogeneity in forest mortality even for adjacent forest patches at 30-m spatial scale (Figure 3a). Previous modeling studies have suggested the role of ecosystem heterogeneity in determining tropical forest responses to water stress (Levine et al., 2016; Longo et al., 2018); however, ecosystem models usually simulated at a very coarse grid scale (1°-by-1°), which ignored the fine-scale variations of forest mortality in the real world. The spatial analysis here provides novel observational evidence that ecosystem heterogeneity, in particular variations in ecosystem deciduousness that result from complex interactions of climate, soil, disturbance history, and plant community composition, regulate fine-scale variations in forest mortality. The maps of mortality can also be used to benchmark the carbon cycle models for tropical forests.

Multiple ecophysiological pathways might underlie the revealed biotic regulation of mortality responses to drought. First, ecosystems with low deciduousness need to maintain more leaf area and have higher water demand, thus exacerbating drought stress under water deficit (Schwartz et al., 2019). In addition, biotic disturbances (insect and fungal attack) associated with drought could have disproportionately affected abundant evergreen species (e.g., *Quercus oleoides*) in the study region (Powers et al., 2020). Indeed, when we applied the BRT analysis over spatially moving windows (Figure S21), the results showed that the importance of deciduousness peaked in the northern part, which overlaps with the distribution of *Quercus*

oleoides in the study region. Disentangling the effects of direct water stress and secondary biotic agents on forest mortality remains a recalcitrant issue. However, deciduousness derived from remote sensing products can serve as ecosystem-scale traits for drought resistance in tropical dry forests in a similar way as hydraulic traits related with species-level vulnerability to drought (Choat et al., 2018; Powers et al., 2020).

Topographical heterogeneity also modulated spatial variations in drought-induced forest mortality. The effects of elevation and slope (Figure 5c, d) are not due to topographical effects on local hydrology because topographic wetness index was also included in the model and had little effects (Figure 5h). We expect forests at higher elevations to show larger mortality responses to high temperature and low moisture during the ENSO droughts because trees at higher elevations are more adapted to lower temperature and vapor pressure deficit (Anderegg & HilleRisLambers, 2016; Fadrique et al., 2018). However, our results show that the mortality sensitivity to drought stress became lower at higher elevation due to increases in baseline forest mortality under no drought stress (Figure 4). It is likely because key soil parameters and vegetation structure change along with elevation (e.g., soil depth decreases, tree density increases) that could enhance baseline forest mortality (Hulshof et al., 2020; Lugo & Scatena, 1996). Because the field sites used are mainly established at relative low elevation (Table S2) and forest mortality observations at high elevation are lacking, a more mechanistic understanding of the elevation effects on drought-driven mortality requires long-term forest census or control experiments along elevation gradients, especially for high land forests.

4.3 | Opportunities and challenges for understanding ecosystem resilience

Temporal autocorrelation of high-frequency variability in Landsat EVI closely associated with ecosystem resilience is the most robust metric for forest mortality. The enhanced data availability on forest biomass mortality rates reveals the role of ecosystem heterogeneity in determining mortality sensitivity to drought in the study regions, calling for consideration of these environmental factors when assessing the vulnerability of tropical forest ecosystems. Rapid development of commercial (e.g., Planet Inc.) and open access (Landsat and Sentinel) high spatial and temporal resolution remote sensing products provide a new era and opportunity for patterns and mechanisms of tree mortality in response to environmental variability, complementing other efforts to monitor forest biomass changes such as GEDI (Global Ecosystem Dynamics Investigation) (Dubayah et al., 2020). Fine-scale forest mortality maps based on remote sensing, together with long-term field plot networks (Brienen et al., 2015; Hubau et al., 2020), can offer a new perspective on forest resistance under extreme drought and constrain mortality modules in terrestrial biosphere models (Bugmann et al., 2019).

Meanwhile, application of the method in a variety of biomes other than tropical dry forests (e.g., tropical rain forests, temperate forests, and boreal forests) needs additional evaluation and the best approach for assimilation of diverse remote sensing products across different temporal and spatial scales remains unclear. Overcoming these challenges ultimately requires compilation of more annual census plots at regional or global scale. Coupling field forest drought experiments with ground or satellite remote sensing would be particularly useful to further understand the relations among biomass loss and ecosystem resilience.

ACKNOWLEDGMENTS

We thank funding from Cornell University CALS to X. X., National Science Foundation CAREER grant DEB-1053237 to J.S.P. and U.S. Department of Energy, Office of Science, Terrestrial Ecosystem Science Program, Award DE-SC0014363 for funding the field plots. We thank Roger Blanco and Maria Marta Chavarria for logistical help in the field. N.G.M. was supported by the U.S. Department of Energy's Next Generation Ecosystem Experiment-Tropics project. A.S-A is supported by National Science and Engineering Research Council of Canada (NSERC) – Discovery Grant Program.

CONFLICT OF INTEREST

The authors declare no conflict of interest.

AUTHOR CONTRIBUTIONS

D.H.W. and X.T.X. designed the research, D.P-A, J.S.P., J.B., A.S-A, S.C-R, J.C.C-A, and A.C-O provided field mortality data, D.H.W. collected the data and the performed analyses, D.H.W. and X.T.X. drafted the paper, Y.L.L. and G.G.K. helped with method development in detecting reduced ecosystem resilience, and all authors contributed to the interpretation of the results and to the text.

DATA AVAILABILITY STATEMENT

The data supporting the results of this study are archived in a public repository (https://doi.org/10.6084/m9.figshare.17207741).

ORCID

Donghai Wu https://orcid.org/0000-0002-4638-3743
German Vargas G. https://orcid.org/0000-0003-1738-0014
Jennifer S. Powers https://orcid.org/0000-0003-3451-4803
Nate G. McDowell https://orcid.org/0000-0002-2178-2254
David Medvigy https://orcid.org/0000-0002-3076-3071
Xiangtao Xu https://orcid.org/0000-0002-9402-9474

REFERENCES

Abatzoglou, J. T., Dobrowski, S. Z., Parks, S. A., & Hegewisch, K. C. (2018). TerraClimate, a high-resolution global dataset of monthly climate and climatic water balance from 1958–2015. *Scientific Data*, *5*(1), 1–12. https://doi.org/10.1038/sdata.2017.191

Aleixo, I., Norris, D., Hemerik, L., Barbosa, A., Prata, E., Costa, F., & Poorter, L. (2019). Amazonian rainforest tree mortality driven by climate and functional traits. *Nature Climate Change*, *9*(5), 384–388. https://doi.org/10.1038/s41558-019-0458-0

Allen, C. D., Breshears, D. D., & McDowell, N. G. (2015). On underestimation of global vulnerability to tree mortality and forest die-off from hotter drought in the Anthropocene. *Ecosphere*, *6*(8), 1–55. https://doi.org/10.1890/ES15-00203.1

Allen, K., Dupuy, J. M., Gei, M. G., Hulshof, C., Medvigy, D., Pizano, C., Salgado-Negret, B., Smith, C. M., Trierweiler, A., Van Bloem, S. J., Waring, B. G., Xu, X., & Powers, J. S. (2017). Will seasonally dry tropical forests be sensitive or resistant to future changes in rainfall regimes? *Environmental Research Letters*, *12*(2), 1–15. https://doi.org/10.1088/1748-9326/aa5968

Anderegg, L. D., Anderegg, W. R., & Berry, J. A. (2013). Not all droughts are created equal: Translating meteorological drought into woody plant mortality. *Tree Physiology*, *33*(7), 701–712. https://doi.org/10.1093/treephys/tpt044

Anderegg, L. D. L., & HilleRisLambers, J. (2016). Drought stress limits the geographic ranges of two tree species via different physiological mechanisms. *Global Change Biology*, *22*(3), 1029–1045. https://doi.org/10.1111/gcb.13148

Anderegg, W. R. L., Anderegg, L. D. L., & Huang, C.-Y. (2019). Testing early warning metrics for drought-induced tree physiological stress and mortality. *Global Change Biology*, *25*(7), 2459–2469. https://doi.org/10.1111/gcb.14655

Anderegg, W. R. L., Hicke, J. A., Fisher, R. A., Allen, C. D., Aukema, J., Bentz, B., Hood, S., Lichstein, J. W., Macalady, A. K., McDowell, N., Pan, Y., Raffa, K., Sala, A., Shaw, J. D., Stephenson, N. L., Tague, C., & Zeppel, M. (2015). Tree mortality from drought, insects, and their interactions in a changing climate. *New Phytologist*, *208*(3), 674–683. https://doi.org/10.1111/nph.13477

Ault, T. R. (2020). On the essentials of drought in a changing climate. *Science*, *368*(6488), 256–260. https://doi.org/10.1126/science.aaz5492

Baccini, A., Walker, W., Carvalho, L., Farina, M., Sulla-Menashe, D., & Houghton, R. A. (2017). Tropical forests are a net carbon source based on aboveground measurements of gain and loss. *Science*, *358*(6360), 230–234. https://doi.org/10.1126/science.aam5962

Bennett, A. C., McDowell, N. G., Allen, C. D., & Anderson-Teixeira, K. J. (2015). Larger trees suffer most during drought in forests worldwide. *Nature Plants*, *1*(10), 1–5. https://doi.org/10.1038/nplants.2015.139

Brando, P. M., Paolucci, L., Ummenhofer, C. C., Ordway, E. M., Hartmann, H., Cattau, M. E., Rattis, L., Medjibe, V., Coe, M. T., & Balch, J. (2019). Droughts, wildfires, and forest carbon cycling: A pantropical synthesis. *Annual Review of Earth and Planetary Sciences*, *47*(1), 555–581. https://doi.org/10.1146/annurev-earth-082517-010235

Brienen, R. J. W., Phillips, O. L., Feldpausch, T. R., Gloor, E., Baker, T. R., Lloyd, J., Lopez-Gonzalez, G., Monteagudo-Mendoza, A., Malhi, Y., Lewis, S. L., Vásquez Martinez, R., Alexiades, M., Álvarez Dávila, E., Alvarez-Loayza, P., Andrade, A., Aragão, L. E. O. C., Araujo-Murakami, A., Arets, E. J. M. M., Arroyo, L., … Zagt, R. J. (2015). Long-term decline of the Amazon carbon sink. *Nature*, *519*(7543), 344–348. https://doi.org/10.1038/nature14283

Bugmann, H., Seidl, R., Hartig, F., Bohn, F., Brůna, J., Cailleret, M., François, L., Heinke, J., Henrot, A.-J., Hickler, T., Hülsmann, L., Huth, A., Jacquemin, I., Kollas, C., Lasch-Born, P., Lexer, M. J., Merganič, J., Merganičová, K., Mette, T., … Reyer, C. P. O. (2019). Tree mortality submodels drive simulated long-term forest dynamics: Assessing 15 models from the stand to global scale. *Ecosphere*, *10*(2), 1–22. https://doi.org/10.1002/ecs2.2616

Calvo-Rodriguez, S., Sánchez-Azofeifa, G. A., Durán, S. M., Do Espírito-Santo, M. M., & Ferreira Nunes, Y. R. (2021). Dynamics of carbon accumulation in tropical dry forests under climate change extremes. *Forests*, *12*(1), 106. https://doi.org/10.3390/f12010106

Castro, S. M., Sanchez-Azofeifa, G. A., & Sato, H. (2018). Effect of drought on productivity in a Costa Rican tropical dry forest. *Environmental Research Letters*, *13*(4), 1–14. https://doi.org/10.1088/1748-9326/aaacbc

Choat, B., Brodribb, T. J., Brodersen, C. R., Duursma, R. A., López, R., & Medlyn, B. E. (2018). Triggers of tree mortality under drought. *Nature*, *558*(7711), 531–539. https://doi.org/10.1038/s41586-018-0240-x

Cooley, S. S., Williams, C. A., Fisher, J. B., Halverson, G. H., Perret, J., & Lee, C. M. (2019). Assessing regional drought impacts on vegetation and evapotranspiration: A case study in Guanacaste, Costa Rica. *Ecological Applications*, *29*(2), 1–21. https://doi.org/10.1002/eap.1834

Dubayah, R., Blair, J. B., Goetz, S., Fatoyinbo, L., Hansen, M., Healey, S., Hofton, M., Hurtt, G., Kellner, J., Luthcke, S., Armston, J., Tang, H., Duncanson, L., Hancock, S., Jantz, P., Marselis, S., Patterson, P. L., Qi, W., & Silva, C. (2020). The Global Ecosystem Dynamics Investigation: High-resolution laser ranging of the Earth's forests and topography. *Science of Remote Sensing*, *1*, 1–14. https://doi.org/10.1016/j.srs.2020.100002

Elith, J., Leathwick, J. R., & Hastie, T. (2008). A working guide to boosted regression trees. *Journal of Animal Ecology*, *77*(4), 802–813. https://doi.org/10.1111/j.1365-2656.2008.01390.x

Fadrique, B., Báez, S., Duque, Á., Malizia, A., Blundo, C., Carilla, J., Osinaga-Acosta, O., Malizia, L., Silman, M., Farfán-Ríos, W., Malhi, Y., Young, K. R., Cuesta C., F., Homeier, J., Peralvo, M., Pinto, E., Jadan, O., Aguirre, N., Aguirre, Z., & Feeley, K. J. (2018). Widespread but heterogeneous responses of Andean forests to climate change. *Nature*, *564*(7735), 207–212. https://doi.org/10.1038/s41586-018-0715-9

Fan, L., Wigneron, J.-P., Ciais, P., Chave, J., Brandt, M., Fensholt, R., Saatchi, S. S., Bastos, A., Al-Yaari, A., Hufkens, K., Qin, Y., Xiao, X., Chen, C., Myneni, R. B., Fernandez-Moran, R., Mialon, A., Rodriguez-Fernandez, N. J., Kerr, Y., Tian, F., & Peñuelas, J. (2019). Satellite-observed pantropical carbon dynamics. *Nature Plants*, *5*(9), 944–951. https://doi.org/10.1038/s41477-019-0478-9

Farr, T. G., Rosen, P. A., Caro, E., Crippen, R., Duren, R., Hensley, S., Kobrick, M., Paller, M., Rodriguez, E., Roth, L., Seal, D., Shaffer, S., Shimada, J., Umland, J., Werner, M., Oskin, M., Burbank, D., & Alsdorf, D. (2007). The Shuttle Radar Topography Mission. *Reviews of Geophysics*, *45*(2), 1–33. https://doi.org/10.1029/2005RG000183

Feldpausch, T. R., Phillips, O. L., Brienen, R. J. W., Gloor, E., Lloyd, J., Lopez-Gonzalez, G., Monteagudo-Mendoza, A., Malhi, Y., Alarcón, A., Álvarez Dávila, E., Alvarez-Loayza, P., Andrade, A., Aragao, L. E. O. C., Arroyo, L., Aymard C., G. A., Baker, T. R., Baraloto, C., Barroso, J., Bonal, D., … Vos, V. A. (2016). Amazon forest response to repeated droughts. *Global Biogeochemical Cycles*, *30*(7), 964–982. https://doi.org/10.1002/2015gb005133

Funk, C., Peterson, P., Landsfeld, M., Pedreros, D., Verdin, J., Shukla, S., Husak, G., Rowland, J., Harrison, L., Hoell, A., & Michaelsen, J. (2015). The climate hazards infrared precipitation with stations-a new environmental record for monitoring extremes. *Scientific Data*, *2*(1), 1–21. https://doi.org/10.1038/sdata.2015.66

Grossiord, C., Buckley, T. N., Cernusak, L. A., Novick, K. A., Poulter, B., Siegwolf, R. T. W., Sperry, J. S., & McDowell, N. G. (2020). Plant responses to rising vapor pressure deficit. *New Phytologist*, *226*(6), 1550–1566. https://doi.org/10.1111/nph.16485

Hartmann, H., Adams, H. D., Anderegg, W. R. L., Jansen, S., & Zeppel, M. J. B. (2015). Research frontiers in drought-induced tree mortality: Crossing scales and disciplines. *New Phytologist*, *205*(3), 965–969. https://doi.org/10.1111/nph.13246

Hilje, B., Calvo-Alvarado, J., Jiménez-Rodríguez, C., & Sánchez-Azofeifa, A. (2015). Tree species composition, breeding systems, and pollination and dispersal syndromes in three forest successional stages in a tropical dry forest in Mesoamerica. *Tropical Conservation Science*, *8*(1), 76–94. https://doi.org/10.1177/194008291500800109

Hirota, M., Holmgren, M., Van Nes, E. H., & Scheffer, M. (2011). Global resilience of tropical forest and savanna to critical transitions. *Science*, *334*(6053), 232–235. https://doi.org/10.1126/science.1210657

Huang, C.-Y., & Anderegg, W. R. L. (2012). Large drought-induced aboveground live biomass losses in southern Rocky Mountain aspen

forests. *Global Change Biology*, *18*(3), 1016–1027. https://doi.org/10.1111/j.1365-2486.2011.02592.x

Hubau, W., Lewis, S. L., Phillips, O. L., Affum-Baffoe, K., Beeckman, H., Cuní-Sanchez, A., Daniels, A. K., Ewango, C. E. N., Fauset, S., Mukinzi, J. M., Sheil, D., Sonké, B., Sullivan, M. J. P., Sunderland, T. C. H., Taedoumg, H., Thomas, S. C., White, L. J. T., Abernethy, K. A., Adu-Bredu, S., … Zemagho, L. (2020). Asynchronous carbon sink saturation in African and Amazonian tropical forests. *Nature*, *579*(7797), 80–87. https://doi.org/10.1038/s41586-020-2035-0

Hulshof, C. M., Waring, B. G., Powers, J. S., & Harrison, S. P. (2020). Trait-based signatures of cloud base height in a tropical cloud forest. *American Journal of Botany*, *107*(6), 1–9. https://doi.org/10.1002/ajb2.1483

Levine, N. M., Zhang, K. E., Longo, M., Baccini, A., Phillips, O. L., Lewis, S. L., Alvarez-Dávila, E., Segalin de Andrade, A. C., Brienen, R. J. W., Erwin, T. L., Feldpausch, T. R., Monteagudo Mendoza, A. L., Nuñez Vargas, P., Prieto, A., Silva-Espejo, J. E., Malhi, Y., & Moorcroft, P. R. (2016). Ecosystem heterogeneity determines the ecological resilience of the Amazon to climate change. *Proceedings of the National Academy of Sciences*, *113*, 793–797. https://doi.org/10.1073/pnas.1511344112

Liu, J., Bowman, K. W., Schimel, D. S., Parazoo, N. C., Jiang, Z., Lee, M., Bloom, A. A., Wunch, D., Frankenberg, C., Sun, Y., O'Dell, C. W., Gurney, K. R., Menemenlis, D., Gierach, M., Crisp, D., & Eldering, A. (2017). Contrasting carbon cycle responses of the tropical continents to the 2015–2016 El Niño. *Science*, *358*(6360), 1–7. https://doi.org/10.1126/science.aam5690

Liu, Y., Kumar, M., Katul, G. G., & Porporato, A. (2019). Reduced resilience as an early warning signal of forest mortality. *Nature Climate Change*, *9*, 880–885. https://doi.org/10.1038/s41558-019-0583-9

Longo, M., Knox, R. G., Levine, N. M., Alves, L. F., Bonal, D., Camargo, P. B., Fitzjarrald, D. R., Hayek, M. N., Restrepo-Coupe, N., Saleska, S. R., Silva, R., Stark, S. C., Tapajós, R. P., Wiedemann, K. T., Zhang, K. E., Wofsy, S. C., & Moorcroft, P. R. (2018). Ecosystem heterogeneity and diversity mitigate Amazon forest resilience to frequent extreme droughts. *New Phytologist*, *219*(3), 914–931. https://doi.org/10.1111/nph.15185

Lugo, A. E., & Scatena, F. N. (1996). Background and catastrophic tree mortality in tropical moist, wet, and rain forests. *Biotropica*, *28*(4), 585–599. https://doi.org/10.2307/2389099

McDowell, N. G., Allen, C. D., Anderson-Teixeira, K., Aukema, B. H., Bond-Lamberty, B., Chini, L., Clark, J. S., Dietze, M., Grossiord, C., Hanbury-Brown, A., Hurtt, G. C., Jackson, R. B., Johnson, D. J., Kueppers, L., Lichstein, J. W., Ogle, K., Poulter, B., Pugh, T. A. M., Seidl, R., … Xu, C. (2020). Pervasive shifts in forest dynamics in a changing world. *Science*, *368*(6494), 1–10. https://doi.org/10.1126/science.aaz9463

McDowell, N., Allen, C. D., Anderson-Teixeira, K., Brando, P., Brienen, R., Chambers, J., Christoffersen, B., Davies, S., Doughty, C., Duque, A., Espirito-Santo, F., Fisher, R., Fontes, C. G., Galbraith, D., Goodsman, D., Grossiord, C., Hartmann, H., Holm, J., Johnson, D. J., … Xu, X. (2018). Drivers and mechanisms of tree mortality in moist tropical forests. *New Phytologist*, *219*(3), 851–869. https://doi.org/10.1111/nph.15027

McDowell, N. G., Michaletz, S. T., Bennett, K. E., Solander, K. C., Xu, C., Maxwell, R. M., & Middleton, R. S. (2018). Predicting chronic climate-driven disturbances and their mitigation. *Trends in Ecology & Evolution*, *33*(1), 15–27. https://doi.org/10.1016/j.tree.2017.10.002

Mitchard, E. T. A. (2018). The tropical forest carbon cycle and climate change. *Nature*, *559*(7715), 527–534. https://doi.org/10.1038/s41586-018-0300-2

Phillips, O. L., van der Heijden, G., Lewis, S. L., López-González, G., Aragão, L. E. O. C., Lloyd, J., Malhi, Y., Monteagudo, A., Almeida, S., Dávila, E. A., Amaral, I., Andelman, S., Andrade, A., Arroyo, L., Aymard, G., Baker, T. R., Blanc, L., Bonal, D., de Oliveira, Á. C. A., … Vilanova, E. (2010). Drought–mortality relationships for tropical forests. *New Phytologist*, *187*(3), 631–646. https://doi.org/10.1111/j.1469-8137.2010.03359.x

Ploton, P., Mortier, F., Réjou-Méchain, M., Barbier, N., Picard, N., Rossi, V., Dormann, C., Cornu, G., Viennois, G., Bayol, N., Lyapustin, A., Gourlet-Fleury, S., & Pélissier, R. (2020). Spatial validation reveals poor predictive performance of large-scale ecological mapping models. *Nature Communications*, *11*(1), 1–11. https://doi.org/10.1038/s41467-020-18321-y

Powers, J. S., Becknell, J. M., Irving, J., & Pèrez-Aviles, D. (2009). Diversity and structure of regenerating tropical dry forests in Costa Rica: Geographic patterns and environmental drivers. *Forest Ecology and Management*, *258*(6), 959–970. https://doi.org/10.1016/j.foreco.2008.10.036

Powers, J. S., Vargas G., G., Brodribb, T. J., Schwartz, N. B., Pérez-Aviles, D., Smith-Martin, C. M., Becknell, J. M., Aureli, F., Blanco, R., Calderón-Morales, E., Calvo-Alvarado, J. C., Calvo-Obando, A. J., Chavarría, M. M., Carvajal-Vanegas, D., Jiménez-Rodríguez, C. D., Murillo Chacon, E., Schaffner, C. M., Werden, L. K., Xu, X., & Medvigy, D. (2020). A catastrophic tropical drought kills hydraulically vulnerable tree species. *Global Change Biology*, *26*, 3122–3133. https://doi.org/10.1111/gcb.15037

Raffa, K. F., Aukema, B. H., Bentz, B. J., Carroll, A. L., Hicke, J. A., Turner, M. G., & Romme, W. H. (2008). Cross-scale drivers of natural disturbances prone to anthropogenic amplification: The dynamics of bark beetle eruptions. *BioScience*, *58*(6), 501–517. https://doi.org/10.1641/b580607

Rogers, B. M., Solvik, K., Hogg, E. H., Ju, J., Masek, J. G., Michaelian, M., Berner, L. T., & Goetz, S. J. (2018). Detecting early warning signals of tree mortality in boreal North America using multiscale satellite data. *Global Change Biology*, *24*(6), 2284–2304. https://doi.org/10.1111/gcb.14107

Rowland, L., da Costa, A. C. L., Galbraith, D. R., Oliveira, R. S., Binks, O. J., Oliveira, A. A. R., Pullen, A. M., Doughty, C. E., Metcalfe, D. B., Vasconcelos, S. S., Ferreira, L. V., Malhi, Y., Grace, J., Mencuccini, M., & Meir, P. (2015). Death from drought in tropical forests is triggered by hydraulics not carbon starvation. *Nature*, *528*(7580), 119–122. https://doi.org/10.1038/nature15539

Saatchi, S., Asefi-Najafabady, S., Malhi, Y., Aragão, L. E., Anderson, L. O., Myneni, R. B., & Nemani, R. (2013). Persistent effects of a severe drought on Amazonian forest canopy. *Proceedings of the National Academy of Sciences*, *110*(2), 565–570. https://doi.org/10.1073/pnas.1204651110

Scheffer, M., Bascompte, J., Brock, W. A., Brovkin, V., Carpenter, S. R., Dakos, V., Held, H., van Nes, E. H., Rietkerk, M., & Sugihara, G. (2009). Early-warning signals for critical transitions. *Nature*, *461*(7260), 53–59. https://doi.org/10.1038/nature08227

Scheffer, M., Carpenter, S. R., Lenton, T. M., Bascompte, J., Brock, W., Dakos, V., van de Koppel, J., van de Leemput, I. A., Levin, S. A., van Nes, E. H., Pascual, M., & Vandermeer, J. (2012). Anticipating critical transitions. *Science*, *338*(6105), 344–348. https://doi.org/10.1126/science.1225244

Schwalm, C. R., Anderegg, W. R. L., Michalak, A. M., Fisher, J. B., Biondi, F., Koch, G., Litvak, M., Ogle, K., Shaw, J. D., Wolf, A., Huntzinger, D. N., Schaefer, K., Cook, R., Wei, Y., Fang, Y., Hayes, D., Huang, M., Jain, A., & Tian, H. (2017). Global patterns of drought recovery. *Nature*, *548*(7666), 202–205. https://doi.org/10.1038/nature23021

Schwartz, N. B., Budsock, A. M., & Uriarte, M. (2019). Fragmentation, forest structure, and topography modulate impacts of drought in a tropical forest landscape. *Ecology*, *100*(6), 1–14. https://doi.org/10.1002/ecy.2677

Staver, A. C., Archibald, S., & Levin, S. A. (2011). The global extent and determinants of savanna and forest as alternative biome states. *Science*, *334*(6053), 230–232. https://doi.org/10.1126/science.1210465

Strogatz, S. H. (2018). *Nonlinear dynamics and chaos with student solutions manual: With applications to physics, biology, chemistry, and engineering*. CRC Press.

van Breugel, M., Ransijn, J., Craven, D., Bongers, F., & Hall, J. S. (2011). Estimating carbon stock in secondary forests: Decisions and uncertainties associated with allometric biomass models. *Forest Ecology and Management*, *262*(8), 1648–1657. https://doi.org/10.1016/j.foreco.2011.07.018

Verbesselt, J., Umlauf, N., Hirota, M., Holmgren, M., Van Nes, E. H., Herold, M., Zeileis, A., & Scheffer, M. (2016). Remotely sensed resilience of tropical forests. *Nature Climate Change*, *6*, 1028–1031. https://doi.org/10.1038/NCLIMATE3108

Wigneron, J.-P., Fan, L., Ciais, P., Bastos, A., Brandt, M., Chave, J., Saatchi, S., Baccini, A., & Fensholt, R. (2020). Tropical forests did not recover from the strong 2015–2016 El Niño event. *Science Advances*, *6*(6), 1–10. https://doi.org/10.1126/sciadv.aay4603

Xu, X., Medvigy, D., Powers, J. S., Becknell, J. M., & Guan, K. (2016). Diversity in plant hydraulic traits explains seasonal and inter-annual variations of vegetation dynamics in seasonally dry tropical forests. *New Phytologist*, *212*(1), 80–95. https://doi.org/10.1111/nph.14009

Yang, X., Xu, X., Stovall, A., Chen, M., & Lee, J.-E. (2021). Recovery: Fast and slow—Vegetation response during the 2012–2016 California drought. *Journal of Geophysical Research: Biogeosciences*, *126*(4), 1–14. https://doi.org/10.1029/2020JG005976

Yang, Y., Saatchi, S. S., Xu, L., Yu, Y., Choi, S., Phillips, N., Kennedy, R., Keller, M., Knyazikhin, Y., & Myneni, R. B. (2018). Post-drought decline of the Amazon carbon sink. *Nature Communications*, *9*(1), 1–9. https://doi.org/10.1038/s41467-018-05668-6

Young, D. J. N., Stevens, J. T., Earles, J. M., Moore, J., Ellis, A., Jirka, A. L., & Latimer, A. M. (2017). Long-term climate and competition explain forest mortality patterns under extreme drought. *Ecology Letters*, *20*(1), 78–86. https://doi.org/10.1111/ele.12711

Zuleta, D., Duque, A., Cardenas, D., Muller-Landau, H. C., & Davies, S. J. (2017). Drought-induced mortality patterns and rapid biomass recovery in a terra firme forest in the Colombian Amazon. *Ecology*, *98*(10), 2538–2546. https://doi.org/10.1002/ecy.1950

SUPPORTING INFORMATION

Additional supporting information may be found in the online version of the article at the publisher's website.

How to cite this article: Wu, D., Vargas G., G., Powers, J. S., McDowell, N. G., Becknell, J. M., Pérez-Aviles, D., Medvigy, D., Liu, Y., Katul, G. G., Calvo-Alvarado, J. C., Calvo-Obando, A., Sanchez-Azofeifa, A., & Xu, X. (2021). Reduced ecosystem resilience quantifies fine-scale heterogeneity in tropical forest mortality responses to drought. *Global Change Biology*, 00, 1–14. https://doi.org/10.1111/gcb.16046